Temporal Relationships of F-Actin Bundle Formation, Collagen and Fibronectin Matrix Assembly, and Fibronectin Receptor Expression to Wound Contraction

Marshall P. Welch, George F. Odland,* and Richard A. F. Clark

Division of Dermatology, Departments of Medicine and Pediatrics, National Jewish Center for Immunology and Respiratory Medicine, Denver, Colorado 80206; and * Departments of Medicine and Biological Structure, University of Washington, School of Medicine, Seattle, Washington 98195

Abstract. Wound contraction can substantially reduce the amount of new tissue needed to reestablish organ integrity after tissue loss. Fibroblasts, rich in F-actin bundles, generate the force of wound contraction. Fibronectin-containing microfibrils link fibroblasts to each other and to collagen bundles and thereby provide transduction cables across the wound for contraction. The temporal relationships of F-actin bundle formation, collagen and fibronectin matrix assembly, and fibronectin receptor expression to wound contraction have not been determined. To establish these relationships, we used a cutaneous gaping wound model in outbred Yorkshire pigs. Granulation tissue filled ~80% of the wound space by day 5 after injury while wound contraction was first apparent at day 10. Neither actin bundles nor fibronectin receptors were observed in 5-d wound fibroblasts. Although fibronectin fibrils were assembled on the surfaces of 5-d fibroblasts, few fibrils coursed between cells. Day-7 fibroblasts stained strongly for nonmuscle-type F-actin bundles consistent with a contractile fibroblast phenotype. These cells expressed fibronectin receptors, were embedded in a fibronectin matrix that appeared to connect fibroblasts to the matrix and to each other, and were coaligned across the wound. Transmission EM confirmed the presence of microfilament bundles, cell-cell and cell-matrix linkages at day 7. Fibroblast coalignment, matrix interconnections, and actin bundles became more pronounced at days 10 and 14 coinciding with tissue contraction. These findings demonstrate that granulation tissue formation, F-actin bundle and fibronectin receptor expression in wound fibroblasts, and fibroblast-matrix linkage precede wound contraction.

FIBRONECTIN and actin interrelationships have been of great interest for many years. Early in the study of fibronectin biology, Ali et al. (1977) observed that adding fibronectin to cultures of transformed fibroblasts induced the formation of actin bundles within the cells and concomitantly changed the cells to a more flattened and elongated morphology. In addition, Ali and Hynes (1977) demonstrated that cytochalasin B addition to fibroblast cultures not only caused the disruption of actin filaments but also caused the release of cell surface fibronectin into the medium. An intimate relationship between actin and fibronectin was further established when extracellular fibronectin and intracellular actin were noted to run parallel with each other (Hynes and Destree, 1978). Subsequent transmission electron microscopy studies demonstrated coaxial alignment of intracellular microfilaments and extracellular fibronectin-containing microfilaments across the plasma membrane of hamster and human fibroblasts (Singer, 1979). Furthermore, the reestablishment of this so-called fibronexus was an early event during the fibronectin-induced restoration of normal morphology in transformed fibroblasts (Singer, 1982). More recently, several laboratories (Tamkun et al., 1986; Chen et al., 1985, 1986; Singer et al., 1988) have demonstrated colocalization of fibronectin receptors of the $\beta 1$ integrin family (Hynes, 1987) with fibronectin fibrils externally and cytoplasmic microfilament bundles, suggesting that the transmembrane fibronectin receptor can bridge the external and internal environments. In collaboration with Singer, we demonstrated that actin and fibronectin coalignments occurred across the plasma membrane of fibroblasts in 7–9-d-old healing cutaneous wounds in guinea pigs (Singer et al., 1984). We postulated that such in vivo fibronexus might tether fibroblasts to each other and to the collagenous matrix to effect transmission of fibroblast contraction across the wound space.

Although a fibronectin-rich matrix is known to be deposited during the 1st and 2nd wk of wound repair (Kurkinen et al., 1980; Grinnell et al., 1981; Clark et al., 1982) and fibroblasts rich in peripheal actin bundles are known to appear in wounds between the 1st and 2nd week of wound repair (Gabbiani et al., 1978; Singer et al., 1984), the precise temporal relationships of these morphogenetic changes to

each other and to wound contraction has not been described. Furthermore, no information exists regarding the expression of fibronectin receptors in fibroblasts during wound repair. If biologic functions such as wound contraction, and by extrapolation tissue contraction in numerous fibrocontractive diseases (Skalli and Gabbiani, 1988), are to be attributed to F-actin–rich fibroblasts and extracellular fibronectin-containing linkages, then the in vivo temporal relationships among these phenomena must be better defined. In this study we demonstrate that a contractile fibroblast phenotype, fibronectin-containing fibrillar connections between F-actin–rich fibroblasts, and fibroblast fibronectin receptor expression occur synchronously during cutaneous wound repair and their development precedes wound contraction.

Materials and Methods

Porcine Cutaneous Wound Protocol

Either male or female domestic white Yorkshire pigs weighing 25–35 lb were obtained from Fichter farms (Ft. Collins, CO). After arrival at our institution the pigs were housed according to the American Association for Accreditation for Laboratory Animal Care (AAALAC) standards, allowed to rest for 3 d, and fed Purina pig chow. In preparation for cutaneous wounding, pigs were anesthetized with 20 mg/kg ketamine and 2 mg/kg xylazine and held at stage 7 anesthesia with halothane and 0_2. At appropriate time points before harvest, full-thickness excisional wounds were placed at 15–20 mm intervals along the central mid-paravertebral and flank areas with a sterile, stainless steel 8-mm punch. Wounds were covered with a semipermeable dressings (Tegaderm; 3-M Corp., Minneapolis, MN) followed by a 4 × 4 open-mesh gauze (Winter, 1962). After the dressings were in place the entire mid-section of the pig was wrapped with Elastikon (Johnson & Johnson, New Brunswick, NJ).

A total of three pigs were used for this study. Each pig had three wounds placed 3, 5, 7, 10, and 14 days before harvest. The wounds at each time point were placed at different cranial-caudal positions to avoid the cranial-caudal effect (Auerbach and Auerbach, 1982). At the time of harvest, pigs were anesthetized as described above and a full-thickness eliptical excision was taken from each covered wound site and adjacent normal skin.

Tissue Processing

Immediately after harvest, the eliptical excisions were bisected vertically into equal halves along the major axis of the elipse with a clean, dry double-edge razor blade. One-half of the tissue specimen was fixed in formalin for Masson trichrome histologic studies. The other half was fixed in an acid-alcohol fixative composed of 96% ethanol, 1% glacial acetic acid, and 3% distilled water for Sirius Red and immunofluorescence studies. The specimens were stored in fixative at 4°C overnight and then embedded in paraffin using a Histomatic 166A (Fisher Scientific, Denver, CO). For paraffin embedding of acid-alcohol fixed tissue, all Histomatic solutions were made fresh in order to avoid contamination.

Paraffin embedded tissue specimens were sectioned at 4-μm intervals with a microtome. The sections were mounted on polylysine-coated slides and oven dried at 59°C. The first complete section from the cut face of formalin fixed specimens was used for Masson trichrome staining so that wound contraction and granulation tissue formation measurements were as near to the central wound plane as possible. For Sirius Red and immunofluorescence studies, the 15 sections from the cut face of the acid-alcohol–fixed specimens were used. Thus these observations were made from sections within a 60-μm vertical plane of the wound center.

Mounted tissue sections were deparaffinized immediately before the staining procedure with two 7-min immersions in xylene, two 3-min immersions in absolute ethanol, and two 1-min rinses in 95% ethanol. The sections were rehydrated with several brief rinses in deionized water and then a 10-min incubation in PBS, pH 7.4.

After deparaffinization, slides to be incubated with antibodies to fibronectin or fibronectin receptor were incubated in 15,000 U/ml testicular hyaluronidase (Sigma Chemical Co., St. Louis, MO) in PBS for 30 min at 37°C. The slides were then given three 10-min washes in PBS. The hyaluronidase pretreatment has been demonstrated to restore fibronectin and other extracellular matrix antigen expression in acid-alcohol, paraffin-embedded tissue sections to the same level as present in frozen tissue sections (Folkvord et al., 1989). Since acid-alcohol fixation preserves tissue architecture far better than freezing tissue, our histochemical technique using fixed, paraffin-embedded specimens can delineate finer details of antigen location than that obtainable in frozen sections.

Quantification of Granulation Tissue Formation and Wound Contraction

The first full section from the formalin-fixed half of each bisected wound specimen was mounted on a polylysine-coated slide and stained with Masson trichrome dye. These sections approximated the plane that vertically transected the center of each wound and therefore were considered optimal for assessment of wound surface area and granulation tissue formation.

Wound surface areas were determined from wound diameter measurements taken at the level of the normal epidermal-dermal junction using a microscopic objective reticule that had been calibrated with a stage micrometer. Since the standard error of the mean (SEM) of measurements from three replicate wounds at each time point was <8% (see Fig. 2), we judged that this method was fairly accurate. Direct wound surface measurements could not be made since the wounds were harvested with the wound dressings intact so as not to disturb the wound surface.

The percent granulation tissue occupying each wound was determined from the same central vertical sections as used for wound diameter measurements. The area of each tissue plane occupied by either granulation tissue or total wound space was determined by tracing the respective areas on a computer controlled electronic digitizer (Tektronix, Inc., Beaverton, OR) with the aid of a camera lucida mounted on a Leitz Dialux 20 microscope. Values were expressed as mean percentages of wound vertical area occupied by granulation tissue ± SEM.

Trichrome-stained slides were viewed and photographed with an Olympus BH-2 microscope with transmitted light and an orange filter. Photomicrographs were taken on a 35-mm Kodak Tri-X Pan film (Eastman Kodak Co., Rochester, NY) and developed in Acufine Developer (Acufine, Inc., Chicago, IL).

Antibody Probes

Antibodies to purified human plasma fibronectin (Furie and Rifkin, 1980) were raised in sheep and isolated as previously described (Clark et al., 1981). Antibody purity was determined by Ouchterlony, immunoelectrophoresis, and Western blots against whole human plasma (Norris et al., 1982; Clark et al., 1985) and ELISA against types I, III, and IV collagen and laminin (Grimwood et al., 1988). Mouse monoclonal anti-human type I procollagen antibodies and rabbit polyclonal antibodies to a synthetic peptide of the integrin $\alpha 5$ chain were kind gifts of J. A. McDonald, St. Louis, MO (McDonald et al., 1986; Roman et al., 1989). Rabbit antiactin antibodies were obtained from Biomedical Technologies, Inc. (Cambridge, MA). Protein A ^{125}I-labeled antiactin IgG bound only actin protein in muscle and nonmuscle cell homogenates ran in SDS–acrylamide gels as judged by immunoblotting techniques. In normal skin tissue sections, these antibodies stained arrector pili smooth muscle cells, myoepithelial cells in eccrine glands, and pericytes around small venules and capillaries. Normal resting epidermal cells and fibroblasts did not stain with this antibody. The monoclonal antibody designated HHF-35 was kindly provided by Allen Gown (University of Washington, Seattle, WA) (Tsukada et al., 1987*a*, *b*). HHF-35 recognizes the alpha isoelectrophoresis variant of actin from skeletal, cardiac, and smooth muscle cells and the gamma variant from smooth muscle cells. HHF-35 does not recognize nonmuscle actin. Rabbit polyclonal antibodies to the fibronectin receptor (integrin $\alpha 5$ $\beta 1$ chains) were a kind gift from James Gailit and Erkki Ruoslahti (LaJolla Cancer Research Center, LaJolla, CA). Antisera to fibronectin receptor complexes were raised in rabbits (Pytela et al., 1987) and adsorbed on a fibronectin Sepharose affinity column to avoid contamination with antifibronectin IgG (Singer et al., 1988). Each antibody solution was titered on acid-alcohol–fixed tissue and the concentration that gave maximal specific fluorescence and minimal background fluorescence was used for these studies (Folkvord et al., 1989).

Immunofluorescence Staining Technique

The avidin-biotin complex immunofluorescence technique was used for these studies. Acid-alcohol–fixed, deparaffinized, appropriately processed tissue specimens were incubated for 1 h at 37°C with a blocking solution containing 20 mg/ml human serum albumin (Calbiochem-Behring Corp.,

La Jolla, CA), 200 μg/ml avidin D (Vector Laboratories, Inc., Burlingame, CA), and 50 μg/ml of IgG fraction from the animal species used as a source of biotinylated second antibody—either rabbit, goat, or horse (Vector Laboratories, Inc.). The slides were then washed three times for 10 min each and one of the following primary antibody solutions were applied: rabbit antiactin IgG antibodies at a 1:20 dilution; rabbit antifibronectin receptor at 1:50 dilution; sheep anti-human fibronectin at 1.2 mg/ml; mouse monoclonal IgG anti-type I procollagen at 1:40 dilution; and mouse monoclonal IgG antivimentin at a 1:10 dilution.

After a 1-h incubation in one of the above antibodies at 37°C, the slides were washed three times in PBS. Subsequently, 5 μg/ml of one of the following biotinylated IgG second antibodies, specific for the primary antibody, was applied: goat anti-rabbit IgG, rabbit anti-sheep IgG, horse anti-mouse IgG (Vector Laboratories, Inc.). The slides were again incubated for 1 h at 37°C, then washed in PBS as previously. The final incubation was in a 20 μg/ml solution of FITC avidin-D for 60 min at 37°C. After a final three 10-min washes in PBS, a coverslip was mounted on each slide using 1% paraphenylenediamine (PPD) in 1:1 glycerol/PBS to retard quenching. In addition, PPD counterstains cells a dull green/orange color. Bright yellow fluorescein fluorescence was easily distinguished from the PPD-counterstain during direct visual examination of the slides. Black and white photomicrographs were exposed so that specific fluorescein fluorescence appeared white and the counter stain appeared dull grey (Folkvord et al., 1989). Slides were viewed and photographed with an Olympus Vanox epifluorescence microscope equipped with a halogen light source, a 490-nm excitation filter, and a 515-nm emission filter.

Results

Temporal Discordance of Granulation Tissue Accumulation and Wound Contraction

Wounds at 3 d after injury contained fibrin clot and blood cells (Fig. 1 *a*). Neither fibroblasts or neomatrix were observed, even at the wound margins. By 5 d after injury, however, marked fibroplasia and neovascularization had formed within the wound space (Fig. 1 *b*). Progressive granulation tissue formation continued over the next 2 d so that most day-7 wounds were completely filled with the new tissue (Fig. 1 *c*). However, no wound contraction was evident at these early time-points. Day-10 wounds were hourglass shaped (Fig. 1 *d*) compared with the cup-shaped outline of early wounds. We interpreted this shape change as an early sign of wound contraction. Day-14 wounds (Fig. 1 *e*) were definitely smaller than day-10 or younger wounds denoting marked wound contraction.

Results obtained from quantitative assessment of granulation tissue formation and wound contraction are shown in Fig. 2. Granulation tissue accumulated rapidly from day 3 (0%) to day 5 (75%) and almost completely filled the wound by day 10 (95%). Although a slight downward trend in wound surface area was noted from day 3 to day 7, significant wound contraction was not apparent until day 10 (Fig. 2). Thus, the morphometric measurements confirmed the visual impression that granulation tissue filled the wound several days before significant wound contraction.

From these data we surmised that fibroplasia and angiogenesis by themselves were insufficient to initiate wound contraction. We then investigated the production and accumulation of collagen in early wounds.

Collagen Matrix Accumulation

The kinetics of extracellular collagen matrix accumulation in granulation tissue was examined with Masson trichrome and Sirius Red staining. Trichrome stained specimens from day-5 wounds contained many randomly oriented fibroblasts but little blue-staining collagen (Fig. 3 *a*). In day-7 wounds, however, bundles of collagen were evident (Fig. 3 *b*). The proportion of collagen bundles appeared higher in the day-10 wounds, and the collagen bundles and fibroblasts appeared coaligned across the wound (Fig. 3 *c*). Quantification of wound collagen accumulation by Sirius Red birefringence demonstrated a fairly linear increase of collagen in day-5 to day-14 wounds (data not shown). Thus, the Sirius Red data confirmed the visual impression of collagen bundle accumulation that was observed in trichrome-stained sections of the same wounds.

The time course of collagen matrix formation (Fig. 3, *a–c*) was compared with the detection of fibroblast intracellular type I procollagen by immunofluorescence (Fig. 3, *d–f*). Granulation tissue fibroblasts in the day-5 wounds stained for procollagen with moderate intensity, in a perinuclear granular pattern (Fig. 3 *d*). Fibroblasts in day-7 wounds stained even stronger for procollagen (Fig. 3 *e*). In contrast, procollagen was not observed in fibroblasts of day-10 (Fig. 3 *f*) and day-14 wounds (not shown). Negative staining for procollagen in the day-10 and day-14 wounds was a consistent experimental finding, occurring in different wounds from the same pig, wounds from different pigs, and on several repeat stainings. The lack of staining was not an artifact of tissue fixation or processing since adjacent sections stained brightly for actin and fibronectin (see Figs. 4 and 7, respectively).

Synchronous Formation of Tightly Compacted Actin Bundles and Wound Contraction

Randomly oriented fibroblasts in the day-5 wounds did not stain for peripheral cytoplasmic actin bundles by polyclonal antiactin antibodies (Fig. 4 *a*). Fibroblasts in the day-7 wounds (Fig. 4 *b*) appeared partially coaligned across the wounds and often stained for F-actin in a pattern of loosely organized peripheral bundles. On transmission electron microscopy, some fibroblasts in 7-d wounds contained microfilament bundles that gave the appearance of frayed ropes (Fig. 5) consistent with the immunofluorescence microscopy observations of loose F-actin bundles in 7-d wound fibroblasts (Fig. 4 *b*). All fibroblasts in day-10 and -14 contracting wounds had tightly compacted peripheral cytoplasmic bundles of actin and were coaligned in arrays parallel with the overlying epidermis as judged by immunofluorescence studies (Fig. 4 *c*) and confirmed by electron microscopy (similar to Fig. 6). The F-actin–rich cells coursing across 7-, 10-, and 14-d wounds were not smooth muscle cells as judged by their lack of staining with a monoclonal antibody to muscle actin (HHF-35)[1] (Fig. 4 *f*). As positive controls for HHF-35 in porcine skin, the following cells stained for muscle F-actin: arterial smooth muscle cells (Fig. 4 *d*), arrector pili cells, myoepithelial cells of eccrine glands (Fig. 4 *e*), and pericytes around new capillaries (Fig. 4 *f*). Granulation tissue fibroblasts in all wounds contained abundant, vimentin-positive, cytoplasmic filaments (not shown). Thus, dense bundles of F-actin formed in wound fibroblasts at the time tissue contraction occurred. These F-actin–rich fibroblasts were coaligned across the wound along the lines of the contractile force.

1. *Abbreviations used in this paper*: HHF-35, a monoclonal antibody to muscle actin; TGF-beta, transforming growth factor-beta.

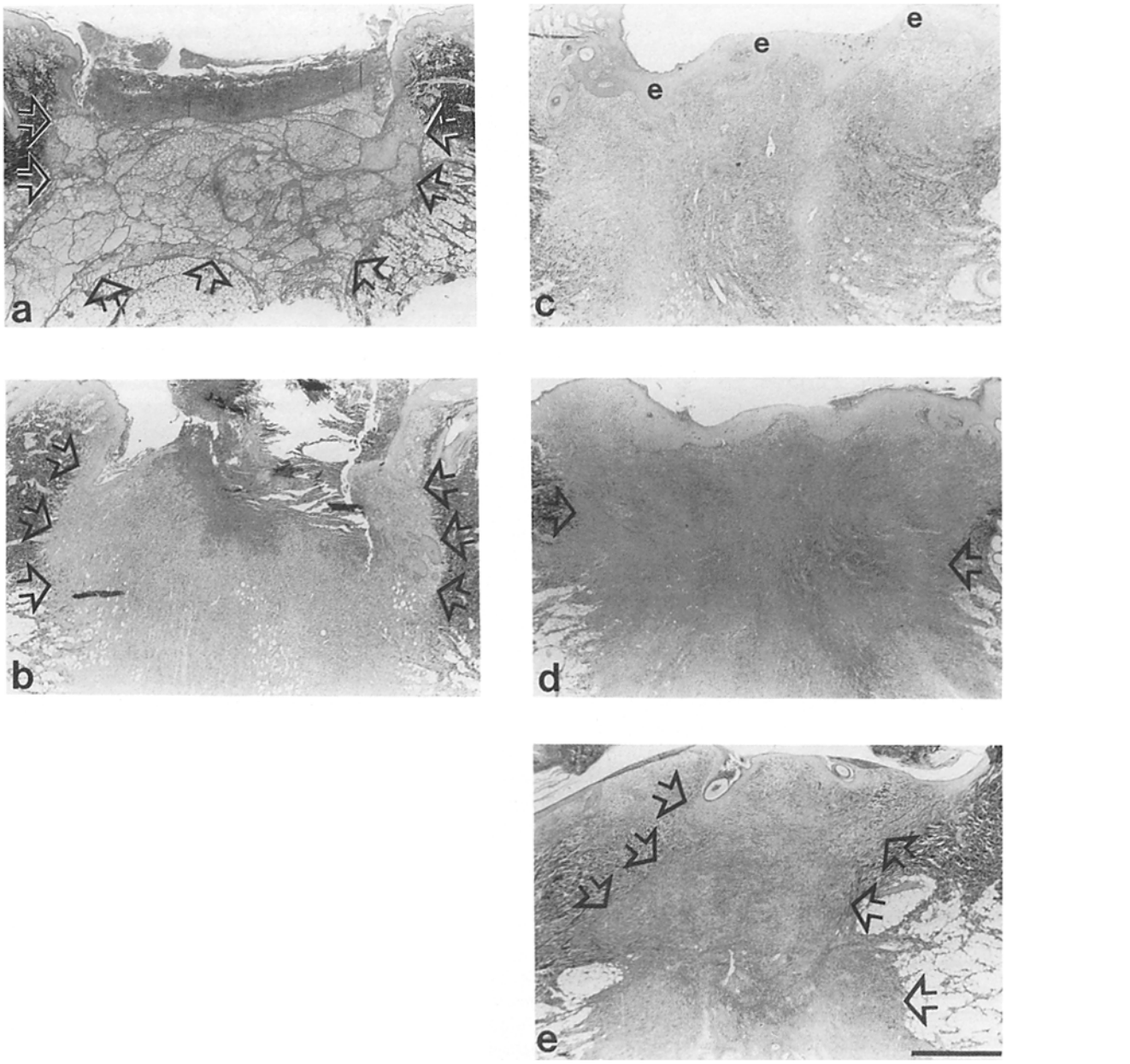

Figure 1. Low power photomicrograph of trichrome-stained skin wounds. (*a*) 3-d wound filled with fibrin clot and blood cells as outlined by arrows. (*b*) 5-d wound in which the wound space is 75% occupied with granulation tissue as outlined by arrows. (*c*) 7-d wound in which the wound space is 95% filled with granulation tissue and the surface repaved with epithelium, marked *e*. (*d*) A 10-d wound in which the wound space is completely filled with granulation tissue. The hourglass shape of the wound margin suggests that wound contraction has begun (*arrows*). (*e*) 13-d wound that has greatly contracted. Arrows outline the wound space. Bar, 1 mm.

Cell–Cell and Cell–Matrix Linkages

Two types of fibroblast linkages were noted in 7-d wounds (Fig. 6 *a*): cell–cell interconnections and cell–matrix links. Cell–cell interconnections occurred at densities along juxtaposing plasma membranes where cytoplasmic microfilaments from the respective cells appeared to insert. A representative example of such cell–cell interconnections is shown at the left-hand end of the fibroblast in Fig. 6 *a* and magnified in Fig. 6 *b*. At other sites along the plasma membrane, intracytoplasmic microfilaments coaligned with extracellular microfilaments forming cell–matrix links (fibronexus). At the right-hand end of the fibroblast shown in Fig. 6 *a* and enlarged in Fig. 6 *c*, the extracellular microfilaments of one of these fibronexus appeared to interdigitate with a bundle of collagen fibrils. Parenthetically, the microfilaments in this fibroblast are more tightly bundled (Fig. 6 *a, arrows*) than the microfilaments shown in Fig. 5, consistent with the variability in F-actin bundle formation observed in 7-d wound fibroblasts with immunofluorescence (Fig. 4 *b*).Many 7-d wound fibroblasts had loose bundles of F-actin that gave a frayed rope or feathered appearance (Fig. 5). This observation correlates with the poorly organized actin bundles seen in 7-d wound fibroblasts with immunofluorescence techniques. In 7- and 9-d guinea pig wounds the actin bundles

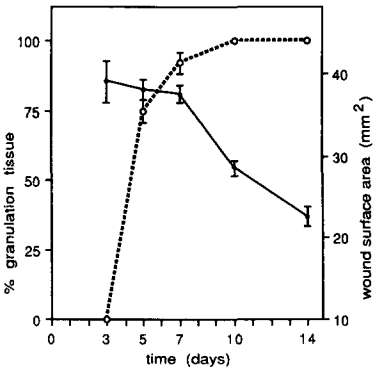

Figure 2. Time course of granulation tissue formation and wound contraction. Percentage of each wound space occupied by granulation tissue was determined morphometrically (see Materials and Methods) and plotted (○). Wound surface areas were calculated from wound diameter measurements (see Materials and Methods) and plotted (●). The data displayed represent the mean of three wound replicates ± SEM that had been placed on a single pig at each time point and are representative of the three pigs studied.

were usually denser and always in a more linear array (Singer et al., 1984) than that shown in Fig. 5. By day 10 the actin bundles in pig wound fibroblasts also consistently showed more compaction and parallel arrays as judged by immunofluorescence (Fig. 4 *c*) and electron microscopy (similar to Fig. 6). Interestingly, guinea pig wounds have already begun to contract by 7 d whereas porcine wounds did not show evidence of contraction until day 10. Thus the morphologic state of the actin bundles appear to relate to tissue tension.

Fibronectin Matrix Assembly

When antibody probes for fibronectin were used to examine day-5 noncontracting wounds, fibronectin fibrils appeared in close proximity to the fibroblasts with only a few fibronectin fibrils obviously interconnecting fibroblasts (Fig. 7 *a*). In the day-7 wounds the fibronectin fibrils were much more extensive and appeared to connect the fibroblasts to each other (Fig. 7 *b*). A similar, extensive fibronectin network that interconnected fibroblasts was also observed in day-10 and day-14 wounds (data not shown). Using antifibronectin antibody probes in conjunction with optical dissection of tissue specimens as described in the legend to Fig. 7, fibronectin fibrils appeared to be confined to the surface of fibroblasts in day-5 wounds (Fig. 7, *c–e*).

Expression of Fibronectin Receptors

A polyclonal antibody to fibronectin receptor (Pitella et al., 1987) revealed weak granular staining within the cytoplasm of fibroblasts at 5 d (Fig. 8 *a*) and moderate granular staining within the cytoplasm at 7 d associated with bright interrupted linear staining along the periphery of cells (Fig. 8 *b*). Although the intracytoplasmic granular staining persisted in 10-d wound fibroblasts, the peripheral staining was absent (not shown). It was notable that pericytes around newly formed capillaries in 5- and 10-d granulation tissue demonstrated a bright peripheral linear pattern with antifibronectin receptor antibodies at a time when fibroblasts stained weakly (see Fig. 8 *a*). Since the polyclonal antibodies to isolated fibronectin receptor recognize both the $\alpha 5$ and $\beta 1$ chains to isolated fibronectin receptor (Singer et al., 1988), it would also recognize other $\beta 1$ integrin receptors including collagen receptors. To further define the integrin receptors expressed in wound fibroblasts, we probed the tissue with rabbit polyclonal antibodies to a synthetic peptide of the integrin $\alpha 5$ chain (Roman et al., 1989). $\alpha 5$ chains were expressed in 7-d wound fibroblasts as a peripheral stitch-work (Fig. 8 *c*) similar to that observed for $\beta 1$ chains (Fig. 8 *b*) but not as perinuclear granules in 5-, 7-, or 10-d wound fibroblasts (not shown for days 5 and 10).

Discussion

In this report we have investigated the temporal relationships of collagen and fibronectin matrix assembly, fibroblast F-actin bundle formation and fibronectin receptor expression, and tissue contraction during repair of excisional cutaneous wounds. Ross and Odland (1968) examined repair of incisional cutaneous wounds ultrastructurally but did not monitor the above parameters. Gabbiani et al. (1978), using immunofluorescence and ultrastructural techniques, documented the presence of F-actin–rich fibroblasts in 10–14-d cutaneous wounds but did not investigate the time course of their appearance. Kurkinen et al. (1980) observed a sequential appearance of fibronectin and collagen during the first 2 wk of fibroplasia into sponge implants but did not relate these events to fibroblast phenotype modulation. In a previous study, we documented that fibronectin-containing microfibrils link F-actin–rich fibroblasts to each other and to collagen bundles in 7–9-d excisional cutaneous wounds (Singer et al., 1984) but we did not investigate the temporal relationships of these phenomena nor did we investigate the expression of integrin receptors.

Collagen Matrix Assembly

Although collagen fibrils appeared in 5-d wounds (Fig. 3 *a*) and increased in 7-d wounds (Fig. 3 *b*), no wound contraction was observed until 10 d (Fig. 2). In our previous ultrastructural observations on 7- and 9-d wounds in guinea pigs, we noted that microfibrillar linkages (fibronexus) coursed between F-actin–rich fibroblasts (myofibroblasts) and collagen bundles (Singer et al., 1984) Thus collagen bundles may be part of a tethering system that links myofibroblasts together and to the wound matrix enabling contractile forces to be transmitted across the wound. Nevertheless a rich collagen matrix as seen in 7-d wounds (Fig. 3 *b*) is clearly not sufficient for wound contraction since a reduction in wound diameter is not observed until day 10.

Wound contraction may affect the collagen matrix through the compaction of collagen bundles. Fibroblasts have been documented to compact collagen bundles in vitro when added to a collagen gel and stimulated to contract (Bell et al., 1981; Bellows et al., 1982; Stopak and Harris, 1982; Grinnell and Lampke, 1984). The further marked increase in collagen bundle density observed at 10 d (Fig. 3 *c*) may be partly attributable to wound contraction effectuating granulation tissue compaction. Supporting this possibility is the lack of type I procollagen staining in day-10 fibroblasts (Fig. 3 *f*) although some collagen synthesis presumably occurred between day 7 and day 10. In fact, small amounts of collagen

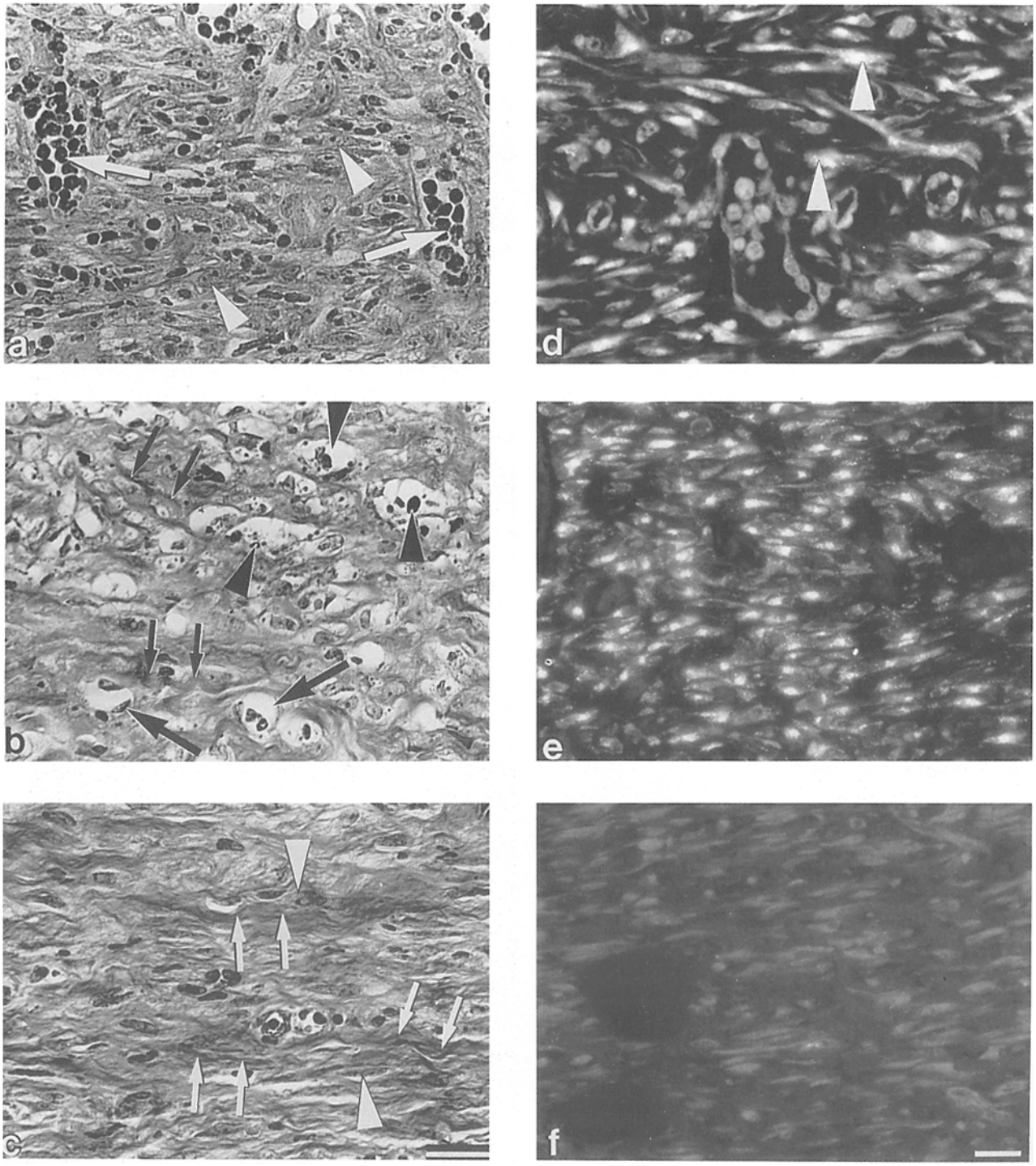

Figure 3. Light and immunofluorescence photomicrographs of collagen accumulation and production, respectively, in day-5 (*a* and *d*), day-7 (*b* and *c*), and day-10 (*c* and *f*) wounds. The left-hand column displays trichrome-stained sections of the same wounds shown in Fig. 2. Each photomicrograph was taken of the wound center. (*a*) Granulation tissue in day-5 wounds contained many randomly oriented fibroblasts (*arrowheads*) and capillary loops (*arrows*). (*b*) In day-7 wounds bundles of collagen were evident (*small arrows*) in addition to capillary loops (*arrows*) and fibroblasts. Vacuoles and debris are secondary to degenerating red blood cells (*arrowheads*). (*c*) Day-10 wounds had a greater amount of collagen (*small arrows*). The collagen bundles (*small arrows*) and fibroblasts (*arrowheads*) appeared coaligned across the wound. The right-hand column displays adjacent wound sections stained with anti-procollagen antibody. (*d*) At day 5 fibrolasts stained moderately for intracellular procollagen in a perinuclear distribution (*arrowheads*). (*e*) Fibroblasts at day 7 stained brightly for procollagen, while day-10 wound fibroblasts (*f*) were negative for procollagen. Bars, 20 μm.

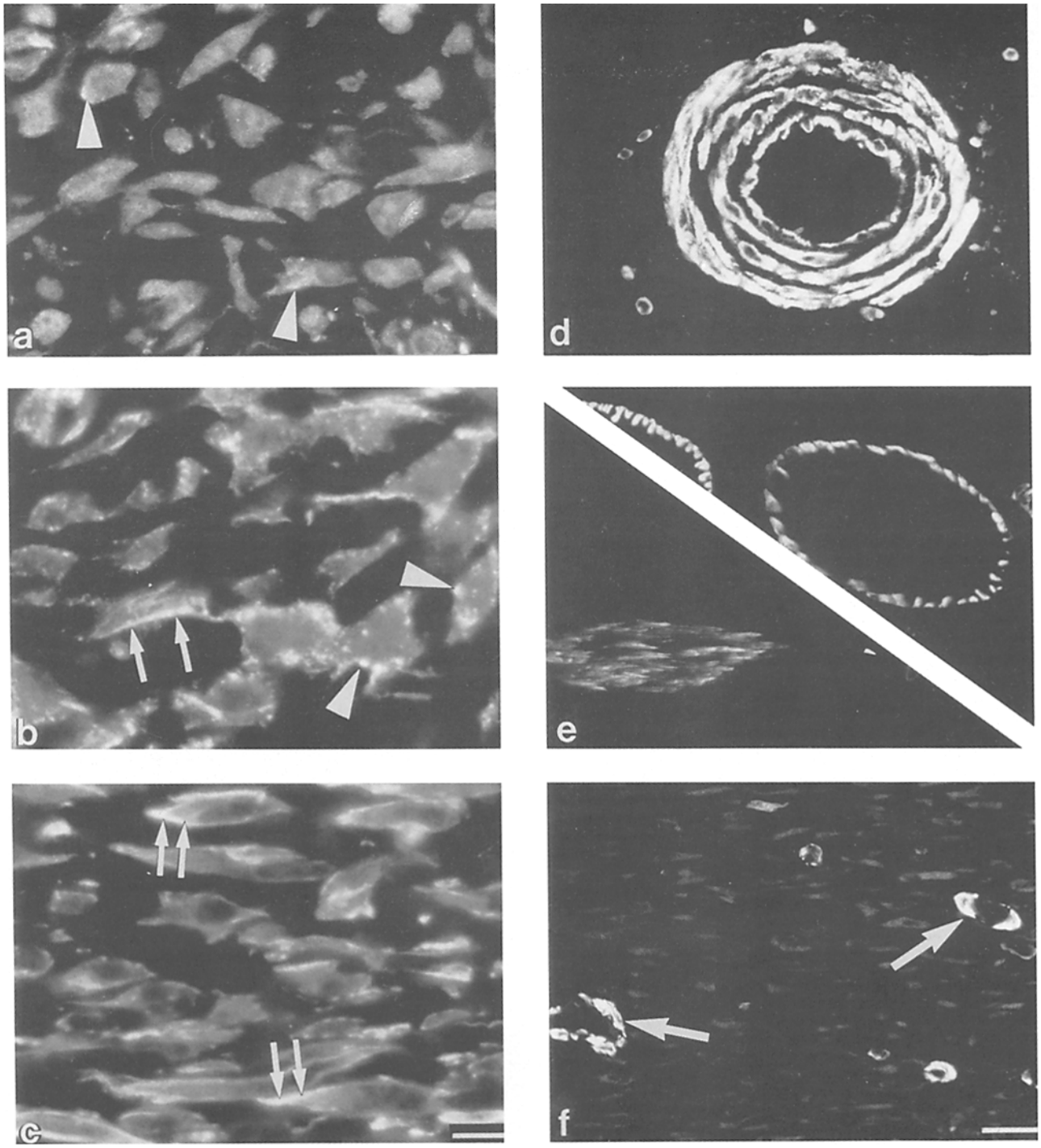

Figure 4. Wound fibroblasts stained with fluorescein-complexed rabbit antiactin antibodies (*a*, *b*, and *c*) or mouse monoclonal antimuscle actin antibodies (*d*, *e*, and *f*). Photomicrographs were taken of the mid-granulation tissue of day-5 (*a*), day-7 (*b*), and day-10 (*c* and *f*) wounds of normal dermis (*d* and *e*). (*a*) Fibroblasts in day-5 wounds were randomly oriented. A few fibroblasts contained weakly staining, small aggregates of actin (*arrowheads*). (*b*) Fibroblasts in day-7 wounds were partially coaligned. Most fibroblasts at this time point contained brightly staining actin aggregates that were disposed along the plasma membrane and appeared in patterns of poorly organized aggregates (*arrowheads*) and organized bundles (*arrows*). (*c*) In 10-d wounds, elongated fibroblasts were aligned parallel to the wound surface. These fibroblasts contained tightly compacted linear arrays of F-actin that were juxtaposed along the plasma membrane and oriented with the long axis of the cell (*arrows*). (*d*) Arteriolar smooth muscle cells stained positive for muscle actin with HHF-35. (*e*) Smooth muscle cells of arrector pili (*bottom*) and myoepithelial cells of sweat glands stained positive with HHF-35 (*top*). (*f*) 10-d wounds stained for muscle actin. Pericytes of small capillaries stain positive with HHF-35 (*arrows*) but fibroblasts were negative. Bars: (*a–c*) 10 μm; (*d–f*) 25 μm.

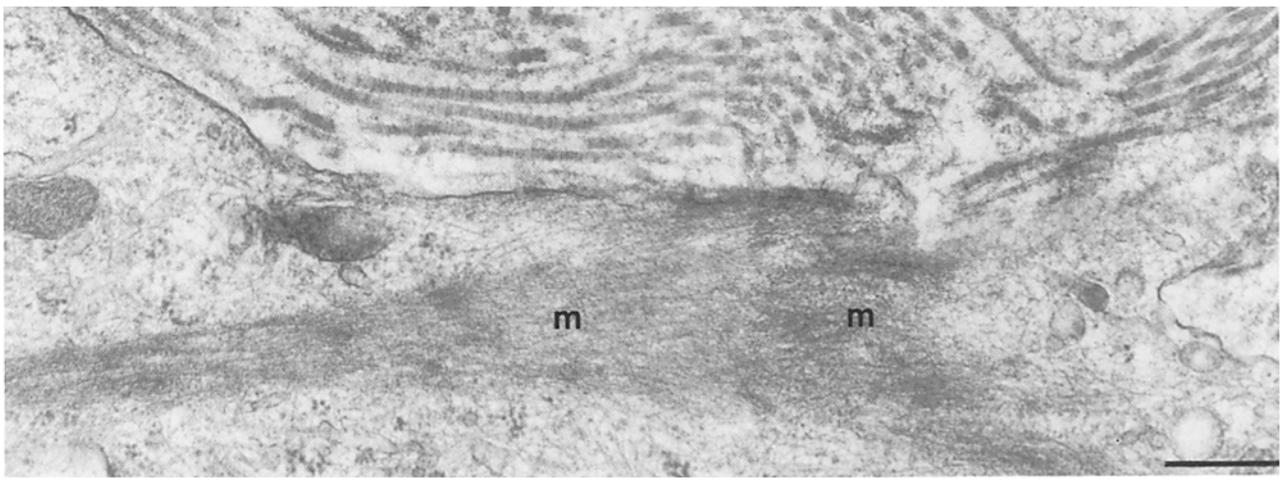

Figure 5. Transmission electron micrograph of a fibroblast from 7-d wound granulation tissue containing microfilaments (*m*) organized in a frayed rope array. Bar, 0.5 μm.

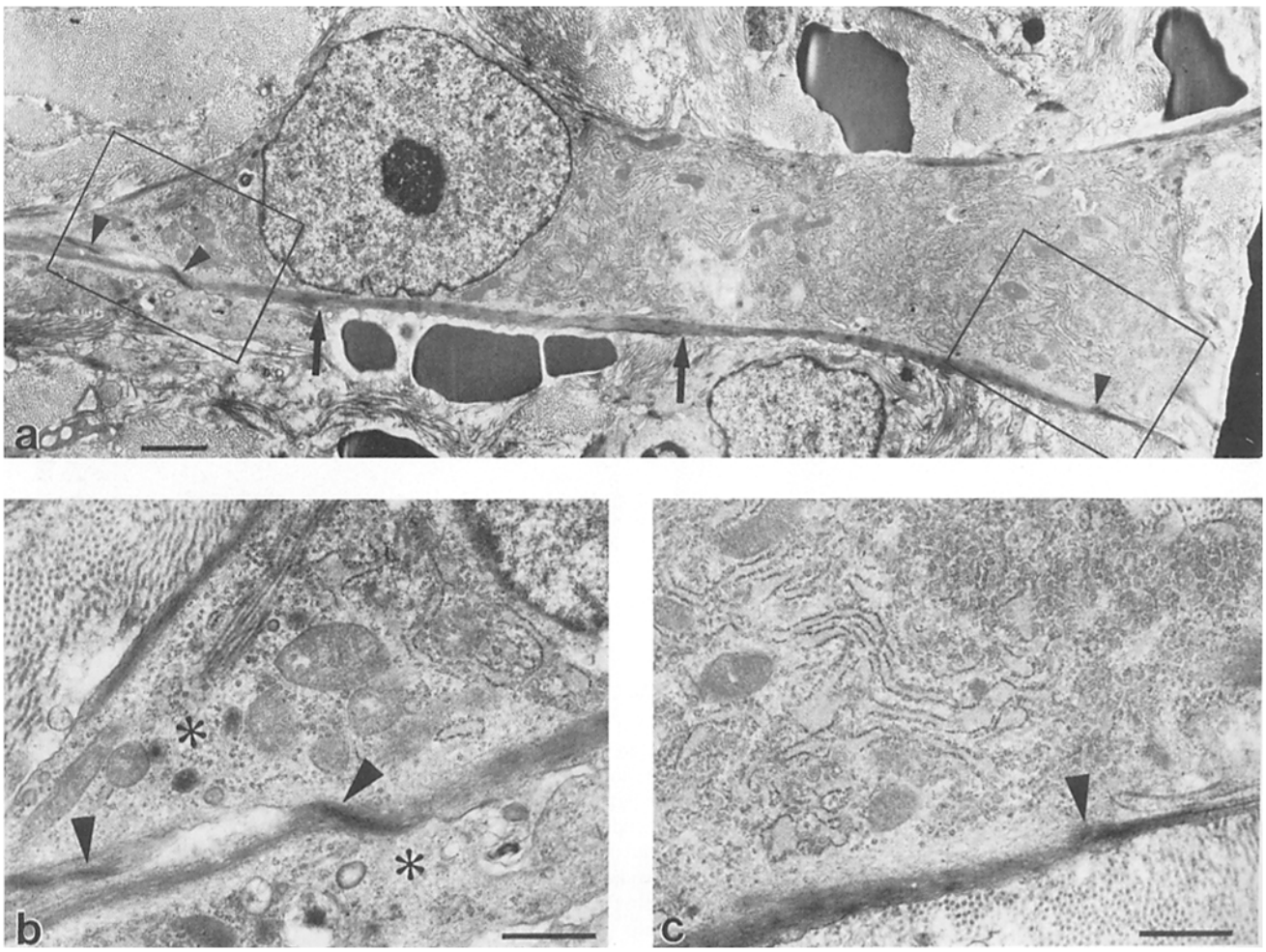

Figure 6. Transmission electron micrograph of a fibroblast in the mid-granulation tissue of a 7-d porcine cutaneous wound. (*a*) The fibroblast contains a well-organized microfilament bundle (*arrows*) coursing along the cytoplasmic face of the plasma membrane. The bundle is engaged in cell–cell (enlarged in *b*) and cell–matrix (enlarged in *c*) linkages (*arrowheads*). The left and right rectangles denote the enlarged areas shown in *b* and *c*, respectively. (*b*) Adjacent fibroblasts (*asterisks*) are linked by a cell–cell adhesion (*arrowheads*) characterized by 10–20-nm intercellular spacing and 60–75-nm-thick cytoplasmic adhesion plaques. (*c*) The intracellular microfilaments appear to be coaligned with extracellular microfilaments to form a fibronexus (*arrowhead*). Bars: (*a*) 2 μm; (*b* and *c*) 1 μm.

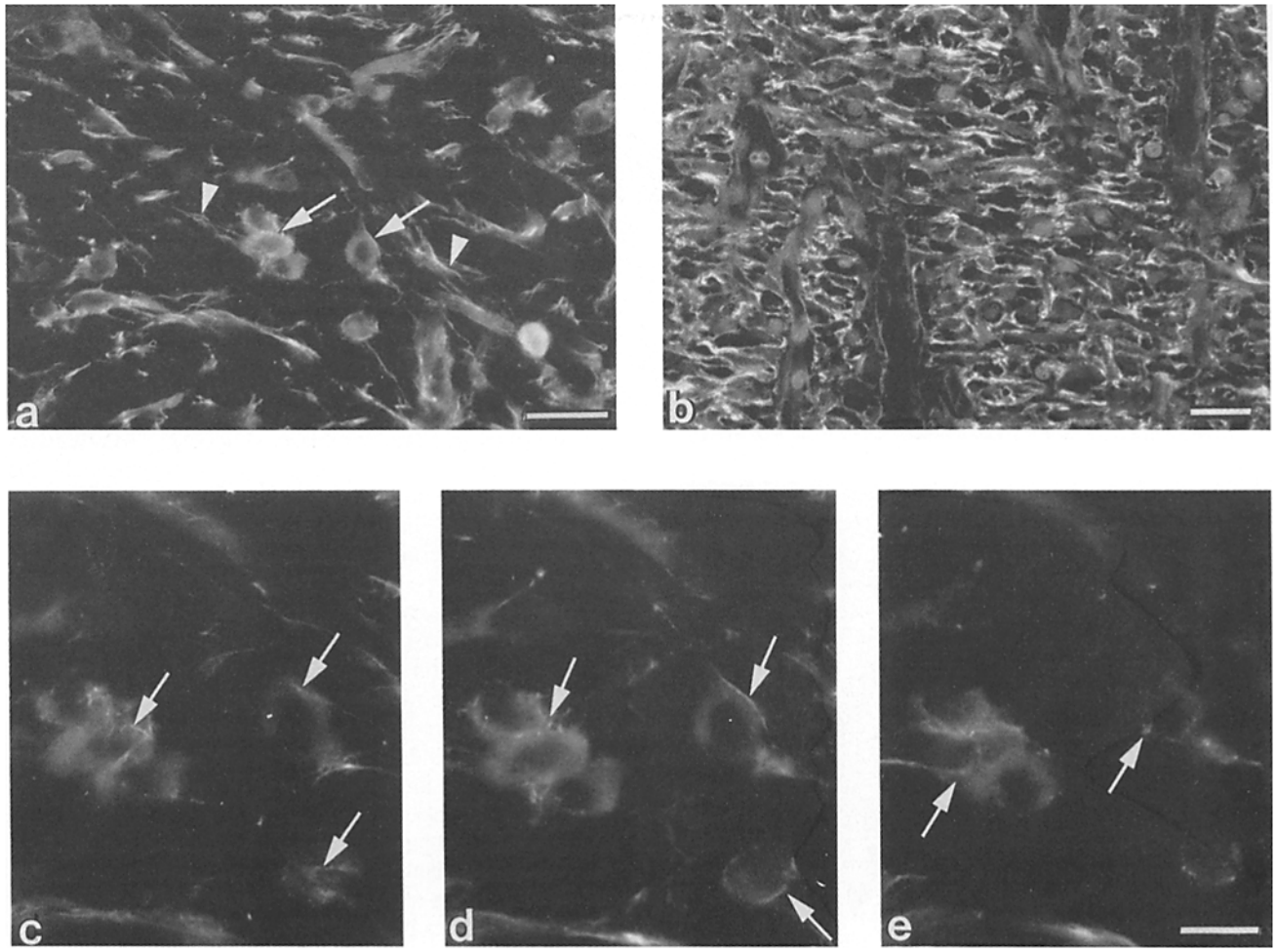

Figure 7. Wound fibroblasts stained with fluorescein-complexed antifibronectin antibodies. Photomicrographs were taken of mid-granulation tissue in day-5 (*a*, *c–e*) and day-7 (*b*) wounds. (*a*) In the day-5 noncontracting wounds, fibronectin fibrils were seen in close proximity to the fibroblasts (*arrows*), and only a few fibronectin fibrils appeared to interconnect fibroblasts (*arrowheads*). (*b*) In the day-7 wounds the fibronectin fibrils were much more extensive and appeared to connect the fibroblasts to each other. A similar but more aligned network of fibronectin interconnected day-10 and day-14 wound fibroblasts (data not shown). (*c–e*) By using a 100× oil immersion objective, photomicrographs were taken of the central field shown in *a*. The microscope micrometer was advanced at 2-μm intervals from the upper surface (*c*) to the middle plane (*d*) and lower surface (*e*) of the specimen. Using this visual dissection of the specimen, fibronectin fibrils were observed to course over the upper surface (*c*, *arrows*) and lower surface (*e*, *arrows*) as well as around the perimeter (*d*, *arrows*) of cells that happened to reside completely within the 4-μm tissue section. Bars: (*a* and *b*) 20 μm; (*c–e*) 10 μm.

synthesis may continue at and beyond day 10 in our wound model that is not detectable by our immunofluorescence technique as Barnes et al. (1975) found that collagen matrix accumulated for many weeks post-wound injury in rodents.

The diminishing rate of collagen synthesis, observed as collagen matrix accumulates, is consistent with in vitro data that demonstrate that fibroblasts plated in collagen gels produced less collagen than fibroblasts plated on plastic (Nusgens et al., 1984). In addition, we have recently found that collagen matrices markedly attenuate fibroblasts' response to transforming growth factor-beta (TGF-beta). Furthermore, in 5- and 7-d wounds TGF-beta is localized to areas where fibroblasts are producing type I procollagen, whereas in 10-d wounds, which contain a dense collagen matrix (Fig 3 *c*), type I procollagen staining was undetectable (Fig. 3 *f*) despite the persistence of TGF-beta (Nielson, L. D., J. M. McPherson, M. P. Welch, J. A. McDonald, and R. A. F. Clark, manuscript submitted for publication). These data are consistent with the notion that TGF-beta is a major positive signal for collagen production (Sporn et al., 1987) while a collagen matrix environment is a major attenuator of this response.

Formation of F-Actin Bundles in Wound Fibroblasts

In recent years wound contraction has been ascribed to "myofibroblasts" that are rich in F-actin bundles, are the most numerous cells in granulation tissue, and are aligned within the wound along the lines of contraction (Skalli and Gabbiani, 1988). By contrast, neither capillaries nor macrophages are aligned along the contraction stress lines. Whether the myofibroblast is an F-actin–rich fibroblast with contractile properties or a smooth muscle cell remained to be clarified. Skalli and Gabbiani (1988) reported from unpublished work

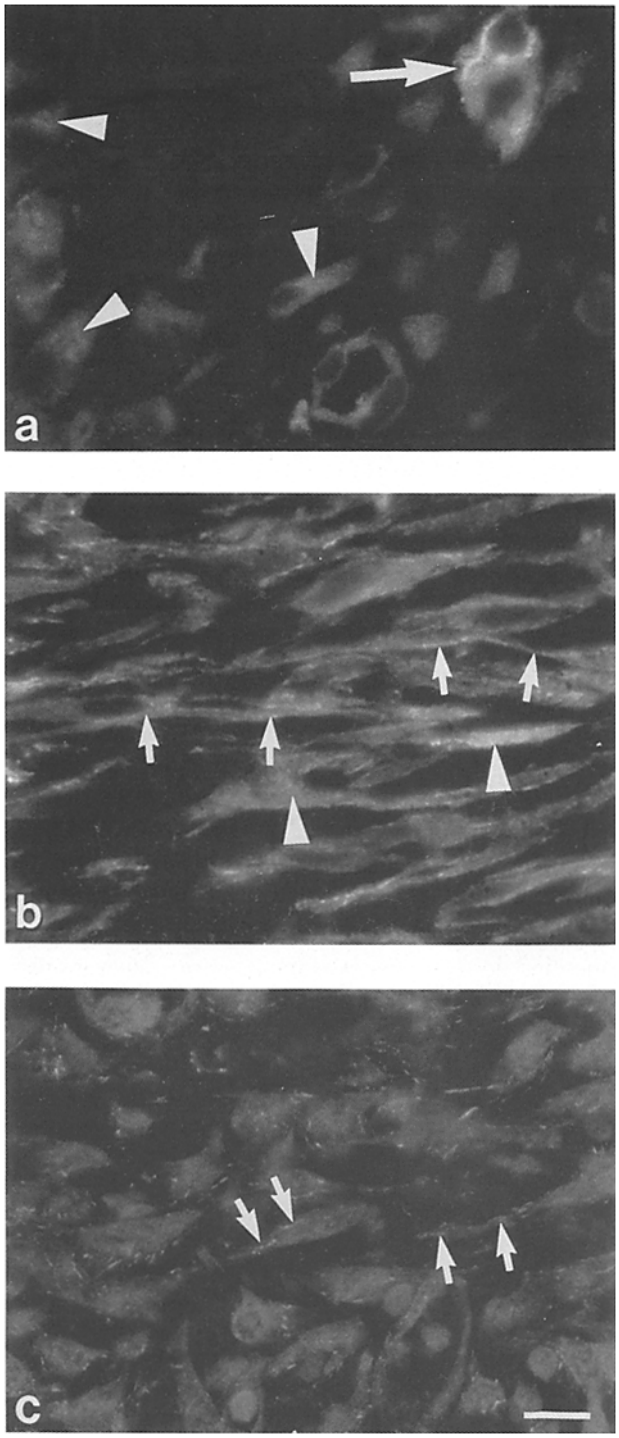

Figure 8. Wound fibroblasts stained with fluorescein-complexed antiintegrin α5 β1 antibodies (*a* and *b*) and an anti-α5 chain antibodies (*c*). Photomicrographs were taken of mid-granulation tissue in day-5 (*a*) and day-7 (*b* and *c*) wounds. (*a*) In day-5 wounds a few fibroblasts stained in a weak perinuclear granular pattern (*arrowheads*) despite bright peripheral staining of pericytes that surrounded some capillaries (*arrow*). (*b*) Striking bright perinuclear granules (*arrowheads*) and peripheral, linear stitches (*small arrows*) were observed in 7-d wound fibroblasts. (*c*) Similar peripheral stitch-work staining (*small arrows*), but no perinuclear granular staining, was seen in 7-d wound fibroblasts with antibodies specific for the integrin α5 chain. Bar, 10 μm.

that granulation tissue myofibroblasts failed to stain with a monoclonal antibody to smooth muscle cell α-actin whereas myofibroblasts in desmoplastic breast tumor stroma were stained positive with the antibody. Furthermore, HHF-35, a monoclonal antibody that recognizes a common determinant on α-actins of striated, cardiac, and smooth muscle cells and on smooth muscle γ-actin, stained myofibroblasts in fibrotic lung and in Dupytren's contracture (Tsukada et al., 1987*b*).

Using HHF-35, we demonstrate in this report that the so-called myofibroblast in granulation tissue failed to stain for muscle actin (Fig. 4 *f*). One interpretation of this apparently conflicting data is that myofibroblasts in fibrotic lung, Dupytren's contracture (Tsukada et al, 1987*b*), and desmoplastic breast carcinoma (Skalli et al., 1986) are derived from smooth muscle cells, while myofibroblasts in wound granulation tissue are derived from fibroblasts (Fig. 4 *f*). Alternatively, myofibroblasts may represent truly pleomorphic cells that can vary their phenotype from smooth muscle cells to fibroblasts (Skalli and Gabbiani, 1988). Since the lineage of this cell type is indeterminate we believe that cells with a morphologic phenotype of myofibroblasts should be described with as much accuracy as possible and that the term myofibroblast be avoided.

Extensive F-actin bundle formation was first observed in granulation tissue fibroblasts of 7-d wounds (Fig. 4 *b*), 2 d after collagen producing fibroblasts occupied the wound space (Fig. 3, *a* and *d*). However, many of the F-actin bundles were loosely formed at 7 d (Fig. 4 *b* and Fig. 5). In contrast, compact linear bundles of F-actin appeared, coursing longitudinally along the peripheral cytoplasm of all fibroblasts, in 10-d wounds (Fig. 4 *c*). These data are consistent with our previous observations that F-actin–rich fibroblasts occurred in guinea pig cutaneous wounds at 7- and 9-d after injury (Singer et al., 1984). Wound contraction occurred at this time (Fig. 2), providing circumstantial evidence that the fibroblasts, rich in F-actin, had contractile properties. In fact, isolated strips of granulation tissue have contractile properties (Gabbiani et al., 1972).

Cell–Cell and Cell–Matrix Linkages

Unified fibroblast-driven contraction of granulation tissue would necessitate molecular connections among fibroblasts and between fibroblasts and the surrounding extracellular matrix. In fact, several types of cell–cell and cell–stroma linkages have been observed in granulation tissue by electron microscopy (Ryan et al., 1974; Gabbiani et al. 1978; Singer et al., 1984). In this study on porcine wounds we have observed two major types of fibroblast linkages in 7-d granulation tissue: a cell–cell linkage first identified by Gabbiani et al. (1978), and a cell–matrix linkage described by Singer et al. (1984). Although Gabbiani et al. (1978) called the cell–cell linkages gap junctions, the cell–cell linkages appear to us more consistent with the cell–cell adhesions described by Chen and Singer (1982). As shown in Fig. 6 *b*, the membrane spacing at the cell–cell junctions is ~10–20 nm. In addition, densities occur along the cytoplasmic face of the junctions and extend into the cell for a distance up to 60 nm. In contrast, cell membranes at gap junctions should only be separated by a 2–3-nm gap. Furthermore, the space between gap junctions should be occupied by rather dense material representing the cylindrical particles that form channels between cells (Revel et al., 1984). Finally, microfilament bundles ap-

peared to insert into the cytoplasmic densities disposed along the cell-cell linkages, an observation compatible with the cell-cell adhesions described by Chen and Singer (1982), but not gap junctions. As described by Singer et al. (1984), the cell-matrix linkages consist of coaligned intracellular microfilaments and extracellular microfilaments. It is postulated that both types of interconnections participate in the transmission of cellular contraction to other tissue components. Thus, the force of wound contraction is presumably generated by the actin bundles in fibroblasts and transmitted to the sides of the wound by cell-cell and cell-stroma links.

Fibronectin Matrix Assembly

Previously we have shown that the cell-matrix linkages in 7- and 9-d guinea pig wounds contained fibronectin (Singer et al., 1984); however, we did not investigate these wounds at earlier time points. Now we have studied 5-d porcine wounds and observed that thin fibronectin fibrils appeared initially on the surface of fibroblasts with a few fibers extending between fibroblasts (Fig. 7, *a*, *c–e*). By 7 d these fibrils had become coarser and had extended between fibroblasts (Fig. 7 *b*) as we had previously observed in guinea pig wounds. Possibly this fibronectin-containing matrix provides a tether to transmit contractile forces across the wound (Singer et al., 1984). Subsequently, in fact, the wounds did contract (Figs. 1 and 2).

Initial assembly of fibronectin fibrils on the fibroblast surface with subsequent extension of those fibrils between cells has also been demonstrated in vitro (McKeown-Longo and Mosher, 1983, 1985; McDonald et al., 1987). A variety of fibroblast surface receptors have been suggested for in vitro fibronectin matrix assembly, including the integrin fibronectin receptor (McKeown-Longo and Mosher, 1985; Spiegel et al., 1986; Roman et al., 1989).

Synchronous assembly of fibronectin matrix and organization of actin bundles in this in vivo study is consistent with the interdependence of extracellular fibronectin assembly and intracellular actin bundle formation previously shown in vitro. Ali et al. (1977) found that the addition of fibronectin to transformed cells that lacked cell surface fibronectin changed their morphology and adhesive properties toward that of untransformed cells, including the development of prominent actin bundles. Ali and Hynes (1977) found that treatment of fibroblasts with cytochalasin B, known to cause disassembly of actin bundles, increased turnover of cell surface fibronectin and inhibited regeneration of cell surface fibronectin after trypsin treatment.

Expression of Fibronectin Receptors

We have observed that F-actin bundle and fibronectin matrix assembly occurred synchronously with fibroblast integrin $\alpha5\beta1$ receptor expression in the cell periphery (Fig. 8). The relative absence of fibronectin receptors during fibroblast ingrowth (Fig. 8 *a*) and their peripheral expression during F-actin bundle formation and extracellular fibronectin matrix assembly (Fig. 8, *b* and *c*) presumably indicates that fibroblasts do not constitutively express fibronectin receptors but rather upregulate their expression when necessary. Alternately, the ingrowing fibroblasts in day-5 wounds may have a uniformly distributed population of fibronectin receptors on their surface, similar to that described for locomoting embryonic fibroblasts in tissue culture (Duband et al., 1988), which would therefore be undetectable in vivo with our immunofluorescence techniques. Once the fibroblasts become stationary, the surface fibronectin receptors may aggregate and become immobile at points of fibronectin fibril assembly (Duband et al., 1988; Roman et al., 1989), rendering them detectable in our in vivo system.

Interestingly, integrin $\beta1$ chains appeared in perinuclear granules of 5-, 7-, and 10-d wound fibroblasts while integrin $\alpha5$ chains only appeared as peripheral stitches in 7-d wound fibroblasts. This observation is consistent with slow post-translational processing and possible intracellular storage of mammalian integrin $\beta1$ chains (Akiyama and Yamada, 1987). Delayed processing has not been observed in integrin $\alpha5$ chain synthesis.

Since the integrin $\beta1$ receptor class also consists of collagen and laminin receptors (Hynes, 1987; Gehlsen et al., 1988), we cannot be certain that integrin receptor expression in 7-d wound fibroblasts is limited to the fibronectin receptor. Since an abundant fibronectin and collagen matrix is being assembled at this time it seems reasonable to assume both the fibronectin and collagen receptors are being expressed as cell surface handles by which fibroblasts can grasp the newly formed matrix proteins.

The stimulus for integrin receptor expression may be TGF-beta since previous in vitro studies demonstrate that TGF-beta can induce fibronectin and collagen receptors in human fibroblasts (Ignotz and Massague, 1987; Roberts et al., 1988; Heine et al., 1989). Supporting this possibility is the fact that TGF-beta is present at sites of fibroplasia in 7-d cutaneous porcine wounds (Nielson, L. D., J. M. McPherson, M. P. Welch, J. A. McDonald, and R. A. F. Clark, manuscript submitted for publication). The diminution of integrin $\beta1$ receptors in the periphery of day-10 wound fibroblasts was unexpected and unlikely to be secondary to nonspecific antigen masking since integrin $\beta1$ receptors were visualized consistently around capillary pericytes in the granulation tissue of day-5, -7, and -10 wounds. Further studies will be necessary to determine the fate of fibronectin receptors during wound contraction.

Hypothetical Model for Fibroplasia and Wound Contraction

From the descriptive data presented here and from current knowledge about cultured fibroblasts and the proteins under study, we have developed a hypothetical model for fibroplasia and wound contraction. First fibroblasts are drawn into a wound space, perhaps by fibronectin (Postlethwaite et al., 1981; Albini et al., 1987), platelet-derived growth factor (Seppa et al., 1982), or TGF-beta (Postlethwaite et al., 1987). The migrating fibroblasts do not synthesize large quantities of type I collagen nor do they contain longitudinal bundles of F-actin. However, once fibroblasts completely populate the wound space, they begin to synthesize large quantities of fibronectin and type I collagen, perhaps in response to TGF-beta (Sporn et al., 1987). Initially fibronectin is confined to the fibroblast surface but within a few days linkages are formed between cells. Concomitantly, the fibroblasts express aggregates of fibronectin receptors, form dense bundles of F-actin along the axis of their peripheral cytoplasm, and become elongated and aligned with each other and with the fibronectin/collagen matrix. Type I procollagen synthesis then diminishes despite a persistence of TGF-beta,

possibly as a consequence of collagen matrix attenuation of the TGF-beta response (Nielson, L. D., J. M. McPherson, M. P. Welch, J. A. McDonald, and R. A. F. Clark, manuscript submitted for publication). During these fibroblast phenotypic modulations, wound contraction occurs implying a causal relationship. We, in fact, propose that the fibroblasts extend bidirectionally, pulling the newly deposited connective tissue matrix in and around themselves. Since the newly formed extracellular matrix is linked together and to the surrounding tissue, the tension exerted on the matrix draws the surrounding tissue inward and wound contraction results.

We appreciate the superb typing assistance of Peggy Hammond and Ruth Ann Hobbie and the expert photo illustration work of Mr. Barry Silverstein. We are grateful to Marcia Usui (Department of Biological Structure, University of Washington, Seattle, WA) for all of the preparative technology and printing of the electron micrographs and for some of the transmission electron microscopy.

These studies were funded by National Institutes of Health grants AM31514, HL27353, the Lester Conrad Research Foundation, and the Scleroderma Foundation. Dr. Marshall Welch was an Immunology Fellow at the National Jewish Center during these studies.

Received for publication 18 April 1989 and in revised form 31 August 1989.

References

Akiyama, S. K., and K. M. Yamada. 1987. Biosynthesis and acquisition of biological activity of the fibronectin receptor. *J. Biol. Chem.* 262:17536–17542.

Albini, A., G. Allavena, A. Melchiori, F. Giancoti, H. Richter, P. M. Comoglio, S. Paroli, G. R. Martin, and G. Tarene. 1987. Chemotaxis of 3T3 and SV3T3 cells to fibronectin is initiated through the cell-attachment site in fibronectin and a fibronectin cell surface receptor. *J. Cell Biol.* 105:1867–1872.

Ali, I. U., and R. O. Hynes. 1977. Effects of cytochalasin B and colchicine on attachment of a major surface protein of fibroblasts. *Biochem. Biophys. Acta.* 471:16–24.

Ali, I. U., V. Mautner, R. Lanza, and R. O. Hynes. 1977. Restoration of normal morphology, adhesion and cytoskeleton in transformed cells by addition of a transformation-sensitive surface protein. *Cell.* 11:115–126.

Auerbach, R., and W. Auerbach. 1982. Regional differences in the growth of normal and neoplastic cells. *Sceince (Wash. DC).* 215:127–134.

Barnes, M. J., L. F. Morton, R. C. Bennett, and A. J. Bailey. 1975. Studies on collagen synthesis in the mature dermal scar in the guinea pig. *Biochem. Soc.* 3:917–920.

Bell, E., H. P. Ehrlich, J. Buttle, and T. Nakatsuji. 1981. Living tissue formed in vitro and accepted as skin-equivalent tissue of full thickness. *Science (Wash. DC).* 211:1052–1054.

Bellows, C. G., A. H. Melcher, and J. E. Aubin. 1982. Association between tension and orientation of periodontal ligament fibroblasts and exogenous collagen fibers in collagen gels in vitro. *J. Cell Sci.* 58:125–138.

Chen, W.-T., and S. J. Singer. 1982. Immunoelectron microscopic studies of the sites of cell–substratum and cell–cell contacts in cultured fibroblasts. *J. Cell Biol.* 95:205–222.

Chen, W.-T., E. Hasegawa, T. Hasegawa, C. Weinstock, and K. M. Yamada. 1985. Development of cell surface linkage complexes in cultured fibroblasts. *J. Cell Biol.* 100:1103–1114.

Chen, W.-T., J. Wang, T. Hasegawa, S. S. Yamada, and K. M. Yamada. 1986. Regulation of fibronectin receptor distribution by transformation, exogenous fibronectin, and sythetic peptides. *J. Cell Biol.* 103:1649–1661.

Clark, R. A. F., H. F. Dvorak, and R. B. Colvin. 1981. Fibronectin in delayed-type hypersensitivity skin reactions. Associations with vessel permeability and endothelial cell activation. *J. Immunol.* 126:787–793.

Clark, R. A. F., R. DellaPella, E. Manseau, J. M. Lanigan, H. F. Dvorak, and R. B. Colvin. 1982. Blood vessel fibronectin increases in conjunction with endothelial cell proliferation and capillary ingrowth during wound healing. *J. Invest. Dermatol.* 79:269–276.

Clark, R. A. F., L. D. Nielsen, S. E. Howell, and J. M. Folkvord. 1985. Non-stratifying cultured keratinocytes synthesize both laminin and fibronectin but deposit only fibronectin in the pericellular matrix. *J. Cell. Biochem.* 28:127–141.

Duband J. L., G. H. Nuckolls, A. Ishihara, T. Haseqawa, K. M. Yamada, J. P. Thiery, and K. Jacobson. 1988. Fibronectin receptor exhibits high lateral mobility in embryonic locomoting cells but is immobile in focal contacts and fibrillar streaks in stationary cells. *J. Cell Biol.* 107:1385–1396.

Folkvord, J. M., A. C. Smith, D. Viders, and R. A. F. Clark. 1989. Optimization of immunohistochemical techniques to detect extracellular matrix proteins in fixed skin specimens. *J. Histochem. Cytochem.* 37:105–113.

Furie, M. B., and D. B. Rifkin. 1980. Proteolytically derived fragments of human plasma fibronectin and their localization within the intact molecule. *J. Biol Chem.* 255:3134–3140.

Gabbiani, G., B. J. Hirschel, G. B. Ryan, P. R. Statkov, and G. Majno. 1972. Granulation tissue as a contractile organ. A study of structure and function. *J. Exp. Med.* 135:719–734.

Gabbiani, G., C. Chapponnier, and I. Huttner. 1978. Cytoplasmic filaments and gap junctions in epithelial cells and myofibroblasts during wound healing. *J. Cell Biol.* 76:561–568.

Gehlsen, K. R., L. Dillner, E. Engvall, and E. Ruoslahti. 1988. The human laminin receptor is a member of the integrin family of cell adhesion receptors. *Science (Wash. DC).* 241:1228–1229.

Grimwood, R. E., J. B. Baskin, L. D. Nielsen, C. F. Ferris, and R. A. F. Clark. 1988. Fibronectin extracellular matrix assembly by human epidermal cells implanted into athymic mice. *J. Invest. Dermatol.* 90:434–440.

Grinnell, F., and C. Lamke. 1984. Reorganization of hydrated collagen lattices by human skin fibroblasts. *J. Cell Sci.* 66:51–63.

Grinnell, F., R. E. Billingham, and L. Burgess. 1981. Distribution of fibronectin during wound healing *in vivo*. *J. Invest. Dermatol.* 76:181–189.

Heine, J., R. A. Ignotz, M. E. Hemler, C. Crouse, and J. Massague. 1989. Regulation of cell adhesion receptors by transforming growth factor-β. Concomitant regulation of integrins that share a common β-1 subunit. *J. Biol. Chem.* 264:380–388.

Hynes, R. O. 1987. Integrins: a family of cell surface receptors. *Cell.* 48:459–554.

Hynes, R. O., and A. T. Destree. 1978. Relationships between fibronectin (LETS protein) and actin. *Cell.* 15:875–886.

Ignotz, R. A., and J. Massague. 1987. Cell adhesion protein receptors as targets for transforming growth factor-β actin. *Cell.* 51:189–197.

Kurkinen, M., A. Vaheri, P. J. Roberts, and S. Stenman. 1980. Sequential appearance of fibronectin and collagen in experimental granulation tissue. *Lab. Invest.* 43:47–51.

McDonald, J. A., T. J. Broekelman, M. I. Matheke, E. Crouch, M. Koo, and C. Kuhn III. 1986. A monoclonal antibody to the carboxyterminal domain of procollagen type I visualizes collagen-synthesizing fibroblasts. *J. Clin. Invest.* 78:1237–1244.

McDonald, J. A., B. J. Quade, T. J. Broekelmann, R. LaChance, K. Forsman, E. Hasegawa, and S. Akiyama. 1987. Fibronectins cell-adhesive domain and an amino-terminal matrix assembly domain participate in its assembly into fibroblast pericellular matrix. *J. Biol. Chem.* 262:2957–2967.

McKeown-Longo, P. J., and D. F. Mosher. 1983. Binding of plasma fibronectin to cell layers of human skin fibroblasts. *J. Cell Biol.* 97:466–472.

McKeown-Longo, P. J., and D. F. Mosher. 1985. Interaction of the 70,000-mol-wt amino-terminal fragment of fibronectin with the matix-assembly receptor of fibroblasts. *J. Cell Biol.* 100:364–374.

Norris, D. A., R. A. F. Clark, L. M. Swigart, J. C. Huff, W. L. Weston, and S. E. Howell. 1982. Fibronectin fragments are chemotactic for peripheral blood monocytes. *J. Immunol.* 129:1612–1618.

Nusgens, B., C. Merrill, C. Lapiere, and E. Bell. 1984. Collagen biosynthesis by cells in a tissue equivalent matrix *in vitro*. *Collagen Rel. Res.* 4:351–364.

Postlethwaite, A. E., J. Keski-Oja, G. Balian, and A. Kang. 1981. Induction of fibroblast chemotaxis by fibronectin. Localization of the chemotaxis region to a 140,000 molecular weight nongelatin binding fragment. *J. Exp. Med.* 153:494–499.

Postlethwaite, A. E., T.Keski-Oja, H. L. Moses, and A. H. Kang. 1987. Stimulation of the chemotactic migration of human fibroblasts by transforming growth factor-β. *J. Exp. Med.* 165:251–256.

Pytela, R., M. D. Pierschbacher, W. S. Argraves, S. Suzuki, and E. Ruoslahti, 1987. Arg-Gly-Asp adhesion receptors. *Methods Enzymol.* 144:475–489.

Revel, J.-P., B. J. Nicolson, and S. B. Yancey. 1984. Molecular organization of gap junctions. *Fed. Proc.* 43:2672–2677.

Roberts, C. J., T. M. Birkenmeier, J. J. McQuillan, S. K. Akiyama, S. S. Yamada, W.-T. Chen, K. M. Yamada, and J. A. McDonald. 1988. Transforming growth factor-β stimulates the expression of fibronectin and both subunits of the human fibronectin receptor by cultured lung fibroblasts. *J. Biol. Chem.* 263:4586–4592.

Roman, J., R. M. LaChance, T. J. Broekelman, C. J. R. Kennedy, E. A. Wagner, W. G. Carter, and J. A. McDonald. 1989. The fibronectin receptor is organized by extracellular matrix fibronectin: implications for oncogenic transformation and for cell recognition of fibronectin matrices. *J. Cell Biol.* 108:2529–2543.

Ross, R., and G. Odland.1968. Human wound repair. II. Inflammatory cells, epithelial-mesenchymal interrelations, and fibrogenesis. *J. Cell Biol.* 39:152–168.

Ryan, G. B., W. J. Cliff, G. Gabbiani, C. Irle, P. R. Statkov, and G. Majno. 1974. Myofibroblasts in human granulation tissue. *Hum. Pathol.* 5:55–67.

Seppa, H. E. J., G. R. Grotendorst, S. I. Seppa, E. Schiffman, and G. R. Martin. 1982. Platelet-derived growth factor is chemotactic for fibroblasts. *J. Cell Biol.* 92:584–588.

Singer, I. I. 1979. The fibronexus: a transmembrane association of fibronectin-containing fibers and bundles of 5nm microfilaments in hamster and human fibroblasts. *Cell.* 16:675–685.

Singer, I. I. 1982. Fibronexus formation is an early event during fibronectin-induced restoration of more normal morphology and substrate adhesion patterns in transformed hamster fibroblasts. *J. Cell Sci.* 56:1–20.

Singer, I. I., D. W. Kawka, D. M. Kazazis, and R. A. F. Clark. 1984. In vivo co-distribution of fibronectin and actin fibers in granulation tissue: immunofluorescence and electron microscope studies of fibronexus at the myofibroblast surface. *J. Cell Biol.* 98:2091–2106.

Singer I. I., S. Scott, D. W. Kawka, D. M. Kazazis, J. Gailit, and E. Rouslahti. 1988. Cell surface distribution of fibronectin and vitronectin receptors depends on substrate composition and extracellular matrix accumulation. *J. Cell Biol.* 106:2171–2182.

Skalli, O., and G. Gabbiani. 1988. The biology of the myofibroblast relationship to wound contraction and fibrocontractive diseases, *In* Molecular and Cellular Biology of Wound Repair. R. A. F. Clark and P. M. Henson, editors. Plenum Publishing Corp., New York. 373–402.

Skalli, O., P. Ropraz, A. Trzeciak, G. Benzonana, D. Gillessen, and G. Gabbiani. 1986. A monoclonal antibody against α-smooth muscle actin: a new probe for smooth muscle differentiation. *J. Cell Biol.* 103:2787–2798.

Spiegel, S., K. M. Yamada, B. E. Hom, J. Moss, and P. H. Fishman. 1986. Fibrillar organization of fibronectin is expressed coordinately by cell surface gangliosides in a variant murine fibroblast. *J. Cell Biol.* 100:721–726.

Sporn, M. B., A. B. Roberts, L. M. Wakefield, and B. de Crombrugghe. 1987. Some recent advances in the chemistry and biology of transforming growth factors beta. *J. Cell Biol.* 105:1039–1045.

Stopak, D., and A. K. Harris. 1982. Connective tissue morphogenesis by fibroblast traction. I. Tissue culture observations. *Dev. Biol.* 90:383–398.

Tamkun, J. W., D. W. DeSimone, D. Fonda, R. S. Patel, C. Buck, A. F. Horwitz, and R. O. Hynes. 1986. Structure of integrin, a glycoprotein involved in the transmembrane linkage between fibronectin and actin. *Cell.* 46:271–282.

Tsukada, T., D. Tippens, D. Gordon, R. Ross, and A. M. Gown. 1987*a*. HHF35, a muscle-actin specific monoclonal antibody. I. Immunocytochemical and biochemical characterization. *Am. J. Path.* 126:51–60.

Tsukada, T., M. A. McNutt, R. Ross, and A. M. Gown. 1987*b*. HHF35, a muscle-actin specific monoclonal antibody. II. Reactivity in normal, reactive, and neoplastic human tissue. *Am. J. Path.* 127:389–402.

Winter, G. F. 1962. Formation of scab and the rate of epithelialization of superficial wounds in the skin of young domestic pig. *Nature (Lond.).* 193:292–294.